Chemical Engineering Journal 164 (2010) 214–220

Contents lists available at ScienceDirect

Chemical Engineering Journal

journal homepage: www.elsevier.com/locate/cej

Activity enhancement of Cu-doped ceria by reductive regeneration of CuO–CeO_2 catalyst for preferential oxidation of CO in H_2-rich streams

A. Razeghi [a], A. Khodadadi [a,*], H. Ziaei-Azad [a], Y. Mortazavi [a,b]

[a] Catalysis and Reaction Engineering Laboratory, University of Tehran, Enghelab Ave., P.O. Box 11365-4563, Tehran, Iran
[b] Nanoelectronics Centre of Excellence, University of Tehran, Tehran, Iran

ARTICLE INFO

Article history:
Received 11 May 2010
Received in revised form 25 July 2010
Accepted 26 July 2010

Keywords:
Regeneration
CO oxidation
Copper
Ceria
Transient

ABSTRACT

Effect of short periods of reduction, in CO and H_2 feed, on regeneration and activity enhancement of a 5.0 wt.% CuO–CeO_2 catalyst for preferential oxidation of CO in a H_2-rich stream at various temperatures is investigated. The catalyst was prepared by a co-precipitation method, calcined at 450 °C for 5 h, and characterized by XRD, FESEM, EDS, BET specific surface area, H_2-TPR and CO_2-TPD. It was found that fine crystallites/amorphous CuO are dispersed on CeO_2 particles with average size of about 33 nm. A gas mixture composed of 1% CO, 40% H_2 and 1% O_2 in N_2 was used as the feed for measurements of the catalyst performance at various temperatures. CO_2 and H_2O were also added to the feed, to study their inhibitive effects on the activity of the catalyst. The activity of the catalyst for CO oxidation significantly enhances after transient reduction in CO and H_2 feed. Higher activity enhancements are observed at lower temperatures and shorter reduction periods. Up to 35% enhancement is observed following 3 min reduction at 100 °C. The most reactive Cu^{1+} species may have formed during the reduction period and regenerates the catalyst leading to higher CO oxidation activities.

1. Introduction

The increase in demand for clean energy based on hydrogen has raised the interest toward fuel cell powered systems for stationary and mobile applications due to their high efficiency along with practically zero emissions of pollutants [1]. Among different types of fuel cells, proton exchange membrane fuel cells (PEMFCs) have gained special interest due to their more convenient operating conditions [2]. The hydrogen feed for PEMFCs is usually produced by a multistep process including catalytic reforming of hydrocarbons or oxygenated hydrocarbons followed by water-gas shift (WGS) reaction. However, the gas stream obtained usually contains 0.5–2.0% CO, 5–10% H_2O and 10–30% CO_2; irrespective of the process applied. Carbon monoxide is a poison for anode catalyst of fuel cell and obviously deteriorates its performance [3]. Therefore, preparation of CO-free hydrogen for fuel cells is of great importance. One of the promising ways to reduce the CO content of effluents from reforming units is preferential oxidation of CO (PROX) in the presence of hydrogen [2–6]. By applying PROX, CO content of the feed can be lowered to less than 10 ppm which is in the range of tolerance limit for anode catalysts. However, the catalyst used in the PROX reaction should exhibit a high catalytic activity and selectivity to minimize consumption of the hydrogen for fuel cells.

Noble metal supported catalysts are often proposed for the PROX process [2–8]. However, the high price and limited resources of noble metals as well as their poor selectivity at very low CO concentration has restricted their application in the PROX process. On the other hand, activity and selectivity of CuO–CeO_2 catalysts in PROX has been shown to be comparable or even superior to noble metal catalysts [7,9]. It has been demonstrated that proper metal–support interaction between copper and cerium oxide result in the synergistic effect which is considered to be responsible for enhancement in activity and selectivity of CO oxidation [10–12]. Thus, with regards to cost and performance, CuO–CeO_2 catalyst may be viewed as a promising catalyst for PROX.

Enhanced oxidation activity (regenerative function) after a short period exposure to a rich (reductive) gas has been reported for Pd/perovskite automotive exhaust catalysts. The most active Pd species in the oxide form diffuses and buries in the perovskite structure and loses its activity in the lean oxidative exhaust gas. When the catalyst is exposed to a rich reductive gas for a short period of time, the Pd is reduced and re-dispersed onto the perovskite surface and gains its high activity for a relatively long period of time [13]. This phenomenon saves the amount of precious metals used for this application.

In this study, the effect of short periods of reduction of a 5.0 wt.% CuO–CeO_2 catalyst on enhancement of CO oxidation activity is investigated for preferential oxidation of CO in a H_2-rich stream at

* Corresponding author. Tel.: +98 21 6696 7792; fax: +98 21 6696 7793.
E-mail address: khodadad@ut.ac.ir (A. Khodadadi).

1385-8947/$ – see front matter © 2010 Elsevier B.V. All rights reserved.
doi:10.1016/j.cej.2010.07.064

various temperatures. Reducing oxygen concentration of the feed to zero, for a short period, induces a sort of regeneration phenomena in the catalyst which in turn improves the catalyst performance.

2. Experimental

2.1. Catalyst preparation

The 5.0 wt.% CuO–CeO_2 catalyst was prepared by a co-precipitation method. Proper amounts of $Ce(NO_3)_3{\cdot}6H_2O$ and $Cu(NO_3)_2{\cdot}3H_2O$ (both from Merck) for a batch of 2.5 g catalyst were dissolved in 400 ml of distilled water. 0.2 M KOH solution was then added drop-wise within 2 h time under vigorous stirring at 80 °C to precipitate the Cu and Ce cations at pH of 10. The sample was kept at 25 °C for 1 h at the same pH, and then filtered and washed with plenty of distilled water to remove the potassium ions followed by further washing with ethanol solution before drying at 120 °C for 2 h. Ethanol is used for dehydration in co-precipitation process which helps to achieve a higher surface area and smaller particle size. The sample was then calcined at 450 °C for 5 h followed by crushing and sieving to a mesh size of 50–120. Also a similar batch of CeO_2 catalyst was prepared by the same method for the supplementary experiments.

2.2. Catalyst characterization

The structure of the catalyst was determined by X-ray powder diffraction (XRD), using a Bruker AXS D8 advanced diffractometer with Cu Kα radiation (λ = 1.5406 Å). The average crystallite size of the catalyst was determined based on Scherrer equation. Field emission scanning electron microscopy (FESEM) and energy dispersive spectroscopy (EDS) were performed using a Hitachi S4160 instrument in order to see the morphology, measure the particle size and analyze composition of the catalyst. BET, H_2-temperature programmed reduction (TPR) and CO_2 temperature programmed desorption (CO_2-TPD) tests were carried out using a Quantachrome CHEMBET-3000 apparatus. BET surface area was measured by N_2 adsorption at the liquid nitrogen temperature. The H_2-TPR experiments were performed on 100 mg of the samples. Prior to the test, catalyst was heated under an O_2 flow up to 450 °C and stayed at this temperature for 0.5 h as a common pretreatment. Afterward, the reactor temperature was lowered down to room temperature by keeping the same flow rate of oxygen. The sample was then reduced by 10 ml/min of 7% H_2 in Ar mixture while the temperature was raised to 1000 °C with a heating rate of 10 °C/min.

The CO_2-TPD experiment was carried out on 100 mg of CuO–CeO_2 sample. Following the same pretreatment adopted for the TPR runs, CO_2 was switched on the sample for 0.5 h. Helium was then fed to the reactor for 0.5 h at room temperature in order to purge out any physically adsorbed CO_2 fractions. The catalyst was then heated to 450 °C at a constant heating rate of 10 °C/min under a flow rate of 10 ml/min of helium.

2.3. Activity and regeneration studies

A schematic diagram of the experimental setup is shown in the Fig. 1. CO, H_2, and either O_2 or N_2 gas streams are mixed to introduce 50 sccm of 1% CO and 40% H_2 (with 1% O_2 or without it) in N_2 to the reactor. Mass flow controllers were used to set the flow rates and a 4-way valve for switching between O_2 and N_2 with the same flow rates for transient experiments.

Oxidation activity of the catalyst for CO conversion in the presence of H_2 was studied in a fixed-bed U-shaped quartz microreactor (4 mm ID) at atmospheric pressure. 0.10 g of the catalyst diluted with the same amount of quartz chips of 50–120 mesh size was used for the oxidation activity measurements. Quartz chips were used to prevent thermal runaway during the transient experiments. The reactor was immersed in a controlled-temperature oil bath. A thermocouple was inserted into the catalyst bed to monitor its temperature. No significant temperature changes was observed, when the reducing CO + H_2 gas was switched to the gas containing O_2.

A mixture of 1% CO, 40% H_2 and 1 vol.% O_2 balanced with N_2 was used as the feed with the total flow rate of 50 sccm in order to investigate the activity of the catalyst for preferential oxidation of CO. The gas space velocity was 30,000 ml g-cat^{-1} h^{-1}. The reactor effluents were analyzed by Shimadzu GC-8A gas chromatograph equipped with a methanizer and FID. The reactor effluent gas was also analyzed on-line with an FTIR spectrometer (Bruker Vector22). The FTIR was equipped with a 0.8 cm ID and 10 cm length gas cell and KBr windows. Transmission mode was applied with a resolution of 5 cm^{-1} in the range of 4000–400 cm^{-1}. There was also a set of valves which allowed by-passing of the reactor feed directly into the GC or FTIR gas cell which provided the direct measurement of the CO concentration in the feed. Using the GC data, a carbon balance based on the total carbon-containing species, with less than 2% error was obtained at steady state PROX conditions. In order to study the effect of in situ reduction on the activity enhance-

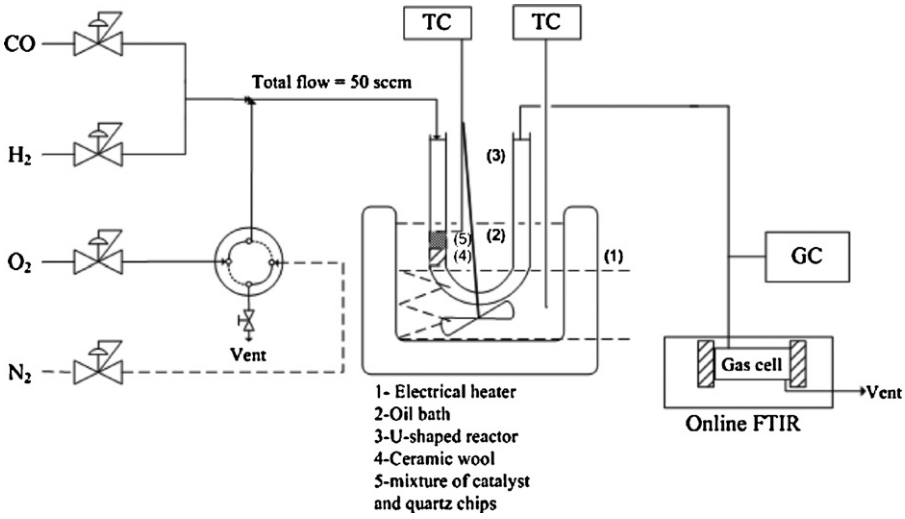

Fig. 1. Schematic diagram of the experimental setup.

ment of the CuO–CeO_2 catalyst, the oxygen stream was switched off for different time intervals at different temperatures. This provided working in transient mode and investigating the regenerative behavior of the catalyst. In that case, mixture of 1 vol.% O_2 in N_2 is switched to N_2 and the former goes to vent while the latter was mixed with the stream of 1% CO and 40% H_2 in order to maintain the total flow rate of 50 sccm during the regeneration time as well. Prior to each regeneration experiment, the sample was heated with the rate of 10 °C/min from the ambient temperature to 220 °C under the feed mixture, and was kept at that temperature for 1 h. Then the reactor was allowed to cool down under the same feed mixture to the desired temperature, at which the stable performance of the catalyst was ensured by 1 h operation.

In order to meet more realistic feed conditions, the effect of CO_2 and H_2O on the activity and regenerative behavior of the catalyst was also investigated by addition of 15 vol.% CO_2 and 5 vol.% H_2O in the feed gas mixture. Water vapor was added by bubbling an N_2 stream in a sparger kept at 60 °C. The gas feedstock was delivered through a tube heated to 80 °C to avoid H_2O condensation.

The CO conversion (%), selectivity of oxygen (%) to oxidized CO and excess oxygen factor (λ), are defined as follows:

$$\text{CO conversion}(\%) = \frac{n_{Co}^{in} - n_{Co}^{out}}{n_{Co}^{in}} \times 100$$

$$O_2 \text{ selectivity}(\%) = \frac{1}{2}\frac{n_{CO}^{in} - n_{CO}^{out}}{n_{O_2}^{in} - n_{O_2}^{out}} \times 100$$

$$\lambda = 2\frac{n_{O_2}^{in}}{n_{Co}^{in}}$$

where n is defined as the number of moles of each component.

In addition, temperature programmed reduction of the fresh catalyst (pre-oxidized in air flow at 300 °C) in 1% CO and 40% H_2 in the absence of oxygen was employed to investigate the redox properties of the catalyst. 0.1 g of the catalyst was placed in the reactor and a mixture of 1% CO and 40 vol.% H_2 was passed over the catalyst bed. The flow rate of the gas mixture was set with mass flow controllers to 10 sccm and the reactor temperature was raised from 50 to 900 °C with a heating rate of 10 °C/min.

3. Results and discussion

3.1. Catalyst characterization

XRD pattern of the fresh 5.0 wt.% CuO–CeO_2 catalyst calcined at 450 °C for 5 h is given in Fig. 2. The diffraction pattern of only CeO_2 crystallites is observed. The reflections in the 2θ range of 15–80°, indicate a cubic, fluorite structure (JCPDS No. 43-1002) with the highest intensity at (1 1 1) plane. There is no peak related to CuO phase, probably due to the fine dispersion and/or amorphous structure of CuO nanoparticles on the surface of ceria. However, the unit cell parameter calculated for both CeO_2 and CuO–CeO_2 samples were 5.45 and 5.42 Å, respectively. This lattice shrinkage may be the consequence of partial incorporation of CuO into the CeO_2 lattice that has been reported for co-precipitation synthesis [11,14].

The average crystallite size of ceria in the catalyst was calculated to be 7.6 nm, using the Scherrer equation. BET surface area of the catalyst is 131 m^2/g. The fine crystallite size along with the high surface area of the catalyst would indicate the proper use of ethanol in the synthesis process already reported [14].

Fig. 3 presents the FESEM micrograph of the catalyst. It seems that 7 nm catalyst particles calculated based on the BET area, are agglomerated to approximately 33 nm sized particles. EDS analysis shows the presence of about 5.8 wt.% CuO in the CuO–CeO_2 catalyst.

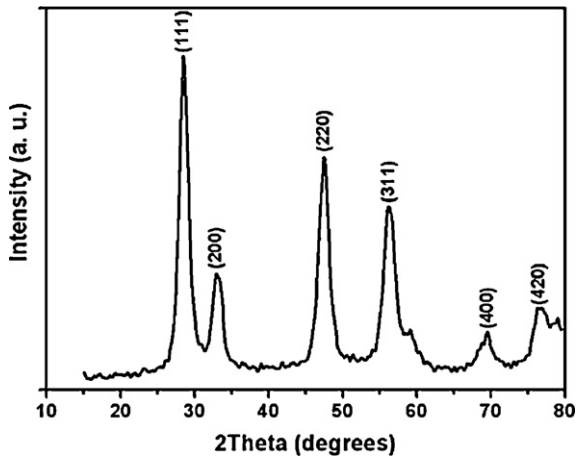

Fig. 2. XRD pattern of fresh CuO–CeO_2 catalyst prepared by co-precipitation method, calcined at 450 °C for 5 h.

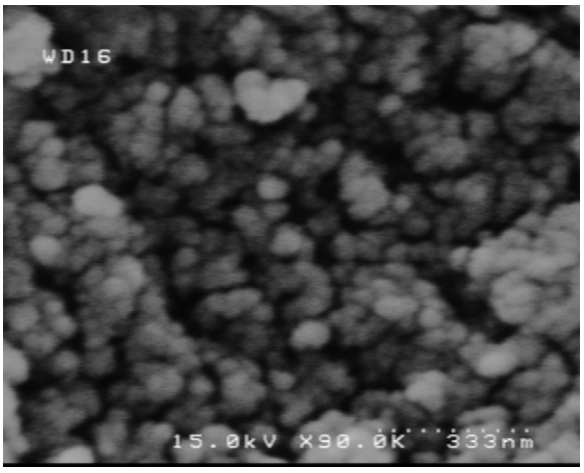

Fig. 3. FESEM micrograph of the CuO–CeO_2 catalyst calcined at 450 °C for 5 h.

Fig. 4 presents the H_2-TPR profiles of the ceria and fresh CuO–CeO_2 catalyst. Two broad reduction ranges are observed in the TPR profile of CeO_2; a 300–600 °C reduction range ascribed to the reduction of surface ceria and a second high temperature range with a maximum at about 900 °C attributed to the reduction of the bulk ceria. Three main reduction peaks are discernable in the H_2-

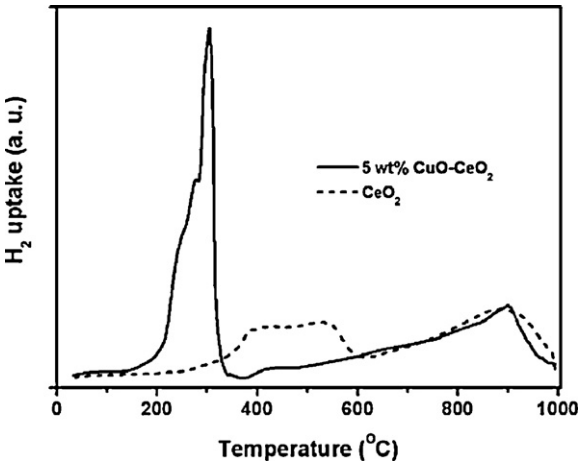

Fig. 4. H_2-TPR of fresh 5.0 wt.% CuO–CeO_2 and CeO_2 catalysts by 10 sccm/min of 7% H_2 in Ar, with the heating rate of 10 °C/min from 50 to 1000 °C.

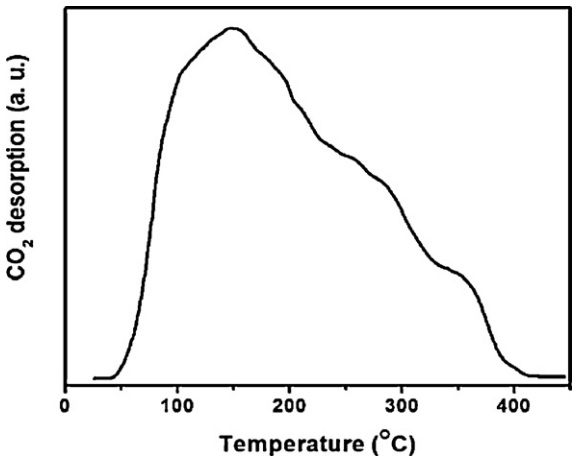

Fig. 5. CO_2-TPD profile of 5.0 wt.% CuO–CeO_2 catalyst from room temperature to 450 °C with the heating rate of 10 °C/min.

TPR profile of the CuO–CeO_2 catalyst, two overlapping peaks in the range of 180–350 °C and the third peak with a maximum at about 900 °C. The overlapping peaks can be attributed to the reduction of the finely dispersed CuO clusters on the surface of ceria as well as further reduction of the bulk CuO phase [14–16]. Furthermore, it has been suggested that a portion of surface ceria reduction can be overlapped with the reduction of CuO [17–19]. CuO may facilitate the reduction of the surface ceria which normally reduces at higher temperatures in the range of 300–600 °C (see Fig. 4). The third broad reduction peak at higher temperatures is related to the reduction of the CeO_2 phase as in the ceria with no CuO.

Fig. 5 presents the CO_2-TPD profile of the CuO–CeO_2 catalyst. The TPD profile shows that CO_2 desorption starts at bout 50 °C and shows a peak at 140 °C with a tail continued to 400 °C.

3.2. Activity and selectivity of the catalyst

Fig. 6 illustrates the CO conversion and O_2 selectivity of 5.0 wt.% CuO–CeO_2 catalyst and pure ceria in the temperature range of 60–210 °C. Ceria shows no detectable CO conversion activity up to 200 °C whereas the catalyst shows an S-shape profile for CO conversion up to the reaction temperature of 165 °C where the CO conversion is 100% (T_{100}) and then the conversion decreases by further increasing the temperature and reaches to 90% at 210 °C. However, selectivity of the catalyst drops below 90% at about

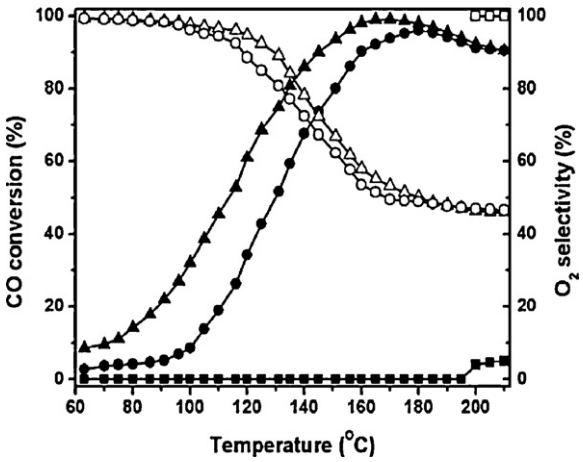

Fig. 6. CO conversion (solid symbols) and O_2 selectivity (open symbols) over CeO_2 (–■–) and 5.0 wt.% CuO–CeO_2 (–▲– H_2O and CO_2 free, –●– with 5 vol.% H_2O and 15 vol.% CO_2).

130 °C. This indicates that at temperatures above 130 °C H_2 oxidation starts to become significant. This is a consequence of the considerable difference in partial pressure of the two reductants [12] as well as higher activation energy of H_2 oxidation, as compared to that of CO [20].

Effects of CO_2 and H_2O added to the feed mixture on the activity and selectivity of the catalyst is presented in Fig. 6. It is observed that addition of CO_2 and H_2O to the hydrogen-rich feed stream increases the T_{50} and T_{90} of CO oxidation by 16 and 14 °C, respectively. It has been reported that blocking effect of CO_2 and H_2O on CO adsorption sites decreases the catalytic activity for CO oxidation [4,21–23]. Furthermore, carbonate formation over reducible metal oxides such as CuO–CeO_2 caused by adsorbed CO_2, is reported to prevent the participation of lattice oxygen and inhibits the oxygen mobility on the ceria support [21,22]. As another reason for activity decline in CO oxidation, the presence of H_2O has been reported to occupy the oxygen vacancies [4]. However, From Fig. 6, it is observed that the selectivity profile does not change drastically by adding H_2O and CO_2 to the feed mixture. This implies that CO and H_2 oxidation rates are decreased to the same amounts. Water-gas shift and reverse water-gas shift reactions were found to be negligible under our experimental temperature [22,23].

3.3. Regeneration of catalyst and enhanced oxidation activity

Fig. 7a shows the transient behavior of the catalyst, when at 115 °C, oxygen in the feed is replaced by N_2 (reducing atmosphere) for a period of 1 or 9 min and then the oxygen is introduced into the reactor, instead of N_2, similar to the steady state operation. Prior to each transient experiment, the stable performance of the catalyst was ensured by 1 h operation at the same temperature. Under reducing atmosphere, the CO conversion gradually decreases to no conversion for the period of 9 min. After the reduction period, when the oxygen is introduced to the feed, CO conversion sharply increases to values higher than that of steady state operation and levels off at longer times on stream. This overshoot of CO conversion after a short period of reduction is called (reductive) regeneration of the catalyst, in this paper. The CO conversion based on CO_2 production for 9 min reduction period is also shown in Fig. 7a. The conversion based on CO_2 production is higher than that based on CO consumption. At longer times the latter sharply decreases to zero at 9 min, while significant production of CO_2 is continued. This may indicate desorption of CO_2 already adsorbed on the catalyst and/or adsorbed CO oxidation, using catalyst lattice oxygen. From the CO_2-TPD profile (see Fig. 5), it is observed that CO_2 desorption mainly occurs in the range of 100–200 °C. This may explain the production of CO_2 in the absence of oxygen, while CO consumption in the gas phase is not detected.

Activity changes of the catalyst after exposure to the reducing atmosphere for different time periods at 115 °C, at which 50% CO conversion occurs at steady state, are shown in Fig. 7b. Maxima of CO conversion enhancements are 12, 13, 12 and 9%, after exposure to the reducing atmosphere for 1, 3, 5, and 9 min, respectively. The CO conversion enhancement gradually decreases, approaching that of steady state. For reduction times of 1–5 min the significant enhancements continues up to 20 min, while for 9 min reduction, the CO conversion reaches more rapidly to its initial value and even negligibly drops below that of steady state. The CO conversion transient behaviors of the catalyst and pure ceria after 3 min exposure to the reducing atmosphere at various temperatures, is presented in Fig. 8a. It is observed that pure ceria does not contribute to activity enhancement of the catalyst. Thus, the presence of CuO is believed to be essential for regenerative behavior of the catalyst. The variation of E_{max} with temperature is shown in Fig. 8b. E_{max} is defined as the difference between the maximum CO conversion in a transient and that of steady state normalized to the steady state

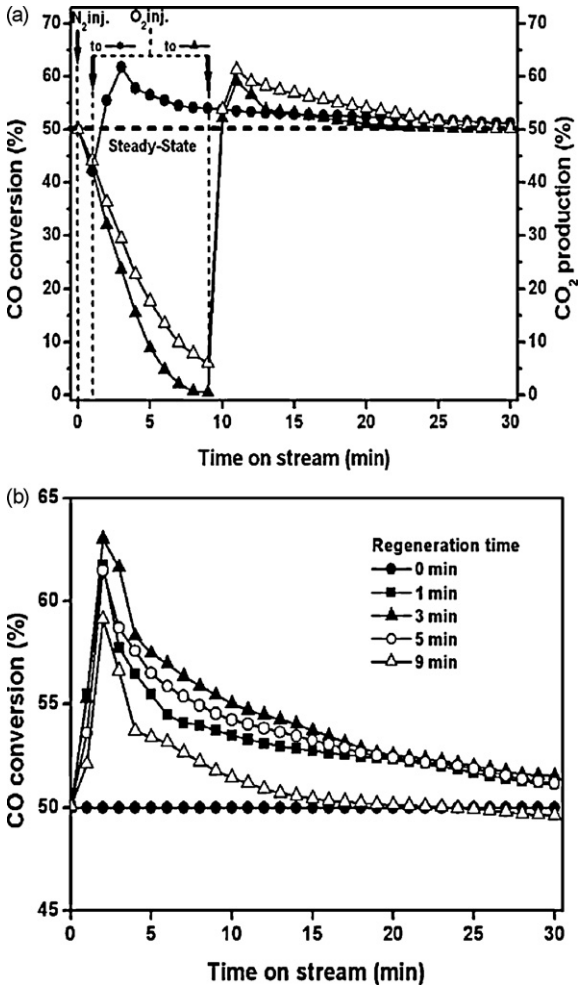

Fig. 7. Reductive regeneration of the catalyst in PROX transient at 115 °C (T_{50}): (a) CO conversion within and after various regeneration times (–●– 1 min, –▲– 9 min) and CO_2 production (–△– 9 min), (b) CO conversion after 0–9 min regeneration times.

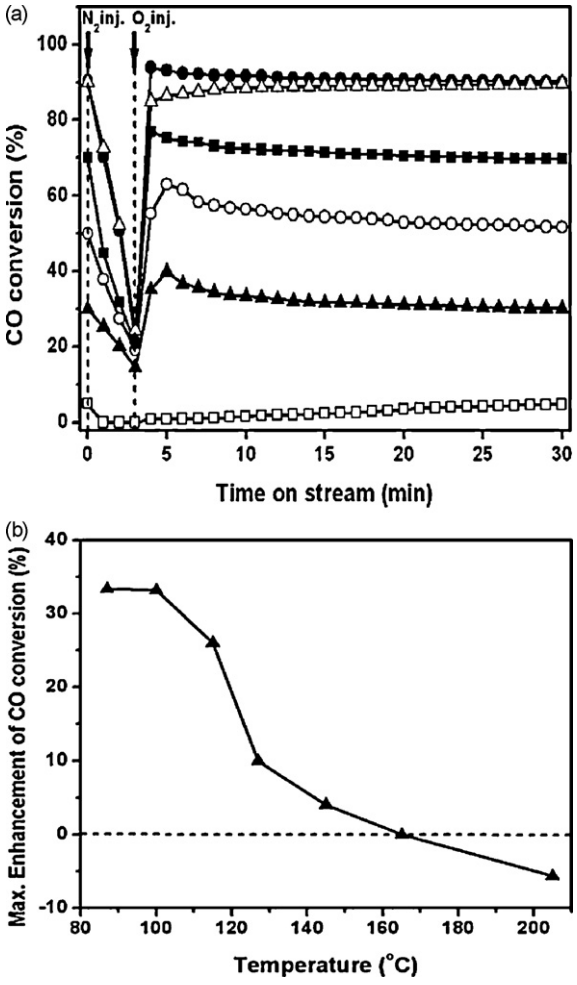

Fig. 8. (a) CO conversion transient as a function of operating temperature during regeneration for 3 min over CeO_2 (–□– 205 °C) and CuO–CeO_2 (–▲– 110 °C, –○– 115 °C, –■– 125 °C, –●– 145 °C, –△– 205 °C) catalyst. (b) Maximum enhancement percentage of CO conversion as a function of operating temperature, after regeneration for 3 min.

one $\{100(CO_{conv.,\,transient,\,max}\text{-}CO_{conv.,\,ss})/CO_{conv.,\,ss}\}$. E_{max} decreases with temperature and the maximum in CO conversion disappears at 165 °C.

The regenerative behavior of the CuO–CeO_2 catalyst in the presence of 5 vol.% H_2O and 15 vol.% CO_2 was investigated at 115 °C and 3 min reduction time. The results are presented in Fig. 9. By adding CO_2 and H_2O to the feed, CO conversion decreases from 50 to 26% at steady state conditions and the maximum of CO conversion is reduced from 63 to 34% after regeneration. Still the regeneration significantly enhances the CO conversion up to about 30%. The overall decline in the catalyst activity in the presence of CO_2 and H_2O may be related to the competitive adsorption of CO_2 and water on active sites that occupy some of the vacancies, on which CO could be adsorbed [21–23].

3.4. Temperature programmed reduction in CO and H_2

Temperature programmed reduction of the 5.0 wt.% CuO–CeO_2 catalyst in the presence of CO and H_2, with the same composition as the microreactor feed during the reductive regeneration period, is presented in Fig. 10. The lattice oxygen of CuO and/or CeO_2 is used for oxidation of CO and H_2 to CO_2 and H_2O, respectively. Water-gas shift reaction may also contribute to CO_2 production. Small amount of methane is produced, most probably by methanation of CO on reduced Cu in the presence of H_2, at temperatures in the range of 400–600 °C [4,24].

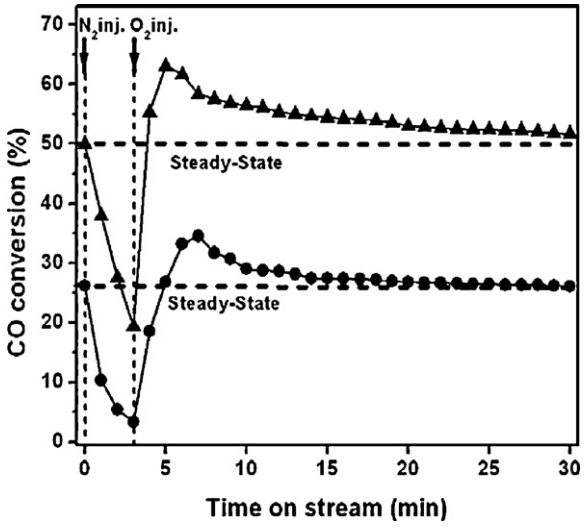

Fig. 9. CO conversion transient at 115 °C during regeneration for 3 min over CuO–CeO_2 catalyst (–▲– H_2O and CO_2 free, –●– with 5 vol.% H_2O and 15 vol.% CO_2).

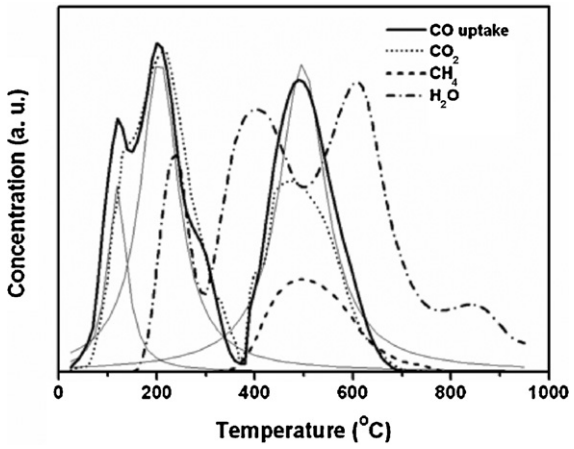

Fig. 10. Temperature programmed reduction of the CuO–CeO_2 catalyst in 10 sccm of 1% CO and 40% H_2 mixture, with heating rate of 10 °C/min.

CO consumption starts at room temperature, when CO adsorbs on highly active Cu species and reduces catalyst. However, CO_2 product desorption is observed at higher temperature in agreement with CO_2-TPD results presented in Fig. 5. Reduction of CuO by hydrogen in H_2-TPR (Fig. 4) starts at about 180 °C, which is much higher than the reduction of CuO in CO and H_2. No significant H_2O production is observed at temperatures lower than 180 °C (Fig. 10). This indicates preferential reduction of CuO by CO at lower temperatures. At higher temperatures both CO and hydrogen may contribute to reduction of CuO and/or CeO_2. It has been shown that CuO is reduced first to Cu_2O and then to Cu^0 [25]. CuO reduction activation energy is much lower than that of Cu_2O [26]. Simultaneous decrease in H_2O and increase in CO_2 production may indicate significant water-gas shift reactions at higher temperatures of about 300 and 500 °C.

The quantitative analysis of CO consumption was studied by the deconvolution of CO uptake peaks in Fig. 10. Two overlapping peaks at 120 and 210 °C together with a high temperature peak at 490 °C are observed for CO uptake in Fig. 10. The low temperature peaks (i.e. 120 and 210 °C) are related mostly to the reduction of Cu species; however, the total amount of CO uptake for these peaks is 831 μmol/g, which is 213 μmol/g higher than the stoichiometric amount for the reduction of Cu species to metallic copper. It is observed that the amount of CO consumption at 120 °C is equal to the required amount for reduction of about 61% of Cu^{2+} into Cu^{1+}, while CO uptake at 210 °C is more than the required amount to reduce the rest of Cu cations into metallic copper. Thus, some reduction of surface ceria should also take into account at low temperatures, which is in agreement with the results reported by Caputo et al. [19]. This excess amount of CO uptake (i.e. 213 μmol/g) is approximately equal to 16% reduction of Ce^{4+} to Ce^{3+} ions.

Comprehension of PROX reaction mechanism is of great importance in understanding the regenerative behavior of CuO–CeO_2 catalysts. Martinez-Arias et al. [3,27–31] have proposed that both copper and cerium cations on the catalyst are engaged in PROX reaction and the interface species between them are the most reactive ones due to the higher liability of the surface oxygen for both copper and cerium. Sedmak et al. [12,32] reported that copper species serve as adsorption sites for carbon monoxide in CuO–CeO_2 matrix. After the CO molecule adsorbs on the catalyst active sites (copper cations), it extracts oxygen from the surface leaving an oxygen vacancy. Simultaneously, Cu^{2+} reduces to Cu^{+} which is subsequently re-oxidized by reduction of Ce^{4+} ions in their vicinity into Ce^{3+}. There are three oxidation states of Cu^0, Cu^{1+} and Cu^{2+} for Cu in the catalyst. CO is easily desorbed from Cu^0 and Cu^{2+}, while it strongly chemisorbs on Cu^{+} sites [32–35]. As a mechanism proposed by Sedmak et al., in the absence of oxygen, the number of surface oxygen vacancies increases due to the reduction of copper species from Cu^{2+} to Cu^{1+}. Consequently, the potential difference between the concentration of oxygen on the surface of the catalyst and in the catalyst bulk is increasing which further result in diffusion of the ceria lattice oxygen to the catalyst surface leading to the formation of bulk oxygen vacancies in cerium oxide [12,32]. This would probably contribute to the redispersion of Cu ions on the surface. As oxygen transfer from bulk to the surface faces mass transfer limitations, the amount of Cu^{1+} cations – which do not reoxidize to Cu^{2+} – increases in the absence of oxygen.

TPR in CO + H_2 may indicate that Cu^{2+} is reduced to Cu^{1+} by CO during the early stages of reduction at low temperatures (Fig. 10). Figs. 6 and 7 show that the reduction of the catalyst during the regeneration time at low temperatures for short periods of time result in significant enhancement of CO oxidation activity of the catalyst. During the regeneration time the Cu^{2+} species may have reduced to the most reactive Cu^{1+} species responsible for the activity enhancement. The Cu^{1+} is re-oxidized to the less reactive Cu^{2+} at longer time of PROX in the presence of O_2-containig gas after the regeneration and the catalyst activity declines (Fig. 7a and b). Regeneration duration as short as 1 min is sufficient to significantly enhance the catalyst oxidation activity. Exposure of the catalyst to the reducing atmosphere of CO + H_2 (with no oxygen) during the regeneration time at higher temperatures and/or for longer periods of time may partially reduce Cu^{2+} more deeply to the less reactive Cu^0 and/or sinter it, leading to lower activity enhancement of the catalyst in PROX.

4. Conclusion

Effect of a short reduction period (regeneration time) on activity enhancement of a CuO–CeO_2 catalyst for preferential oxidation of CO in a H_2–rich stream (PROX) was investigated. CuO was shown to play a key role for PROX as no significant activity and regeneration results is observed for pure ceria. The activity of the catalyst for CO oxidation significantly enhances after the regeneration in CO and H_2 feed (with no O_2) at lower temperatures. The overall activity of the catalyst appreciably declines, when CO_2 and H_2O are added to the feed. Still the regeneration significantly enhances the CO conversion up to about 30%. During the regeneration the Cu^{2+} species may have reduced to the most reactive Cu^{1+} species responsible for the activity enhancement. Exposure of the catalyst to the reducing atmosphere during the regeneration at higher temperatures and/or for longer periods may partially reduce Cu^{2+} more deeply to the less reactive Cu^0 and/or sinter it, which results in lower activity enhancement of the catalyst in the PROX. The regenerative behavior discussed, can be effectively applied in the catalytic reactor for PROX process to reduce the operating temperature and promote the oxidation activity of the catalyst.

References

[1] S. Dunn, Hydrogen futures: toward a sustainable energy system, Int. J. Hydrogen Energy 27 (2002) 235–264.
[2] O. Korotkikh, R. Farrauto, Selective catalytic oxidation of CO in H_2: fuel cell applications, Catal. Today 62 (2000) 249–254.
[3] A. Martinez-Arias, A.B. Hungria, G. Munuera, D. Gamarra, Preferential oxidation of CO in rich H_2 over CuO/CeO_2: details of selectivity and deactivation under the reactant stream, Appl. Catal. B 65 (2006) 207–216.
[4] J.L. Ayastuy, M.P. Gonzalez-Marcos, J.R. Gonzalez-Velasco, M.A. Gutierrez-Ortiz, MnOx/Pt/Al_2O_3 catalysts for CO oxidation in H_2-rich streams, Appl. Catal. B 70 (2007) 532–541.
[5] G. Chen, Q. Yuan, H. Li, S. Li, CO selective oxidation in a microchannel reactor for PEM fuel cell, Chem. Eng. J. 101 (2004) 101–106.
[6] S.H. Oh, R.M. Sinkevitch, Carbon monoxide removal from hydrogen-rich fuel cell feedstreams by selective catalytic oxidation, J. Catal. 142 (1993) 254–262.
[7] G. Avgouropoulos, J. Papavasiliou, T. Tabakova, V. Idakiev, T. Ioannides, A comparative study of ceria-supported gold and copper oxide catalysts for preferential CO oxidation reaction, Chem. Eng. J. 124 (2006) 41–45.

[8] C. Galletti, S. Fiorot, S. Specchia, G. Saracco, V. Specchia, Catalytic performance of Au–TiO_2 catalysts prepared by deposition–precipitation for CO preferential oxidation in H_2-rich gases, Chem. Eng. J. 134 (2007) 45–50.
[9] S. Kandoi, A.A. Gokhale, L.C. Grabow, J.A. Dumesic, M. Mavrikakis, Why Au and Cu are more selective than Pt for preferential oxidation of CO at low temperature, Catal. Lett. 93 (2004) 93–100.
[10] M. Manzoli, R. Di Monte, F. Boccuzzi, S. Coluccia, J. Kaspar, CO oxidation over CuO_x–CeO_2–ZrO_2 catalysts: transient behavior and role of copper clusters in contact with ceria, Appl. Catal. B 61 (2005) 192–205.
[11] P. Ratnasamy, D. Srinivas, C.V.V. Satyanarayana, P. Manikandan, R.S. Senthil Kumaran, M. Sachin, V.N. Shetti, Influence of the support on the preferential oxidation of CO in hydrogen-rich steam reformates over the CuO–CeO_2–ZrO_2 system, J. Catal. 221 (2004) 455–465.
[12] G. Sedmak, S. Hocevar, J. Levec, Kinetics of selective CO oxidation in excess of H_2 over the nanostructured $Cu_{0.1}Ce_{0.9}O_{2-y}$ catalyst, J. Catal. 213 (2003) 135–150.
[13] S. Sartipi, A.A. Khodadadi, Y. Mortazavi, Pd-doped $LaCoO_3$ regenerative catalyst for automotive emissions control, Appl. Catal. B 83 (2008) 214–220.
[14] Z. Liu, R. Zhou, X. Zheng, Preferential oxidation of CO in excess hydrogen over a nanostructured CuO–CeO_2 catalyst with high surface areas, Catal. Commun. 9 (2008) 2183–2186.
[15] M.F. Luo, Y.J. Zhong, X.X. Yuan, X.M. Zheng, TPR and TPD studies of CuO/CeO_2 catalysts for low temperature CO oxidation, Appl. Catal. A 162 (1997) 121–131.
[16] M.F. Luo, Y.P. Song, X.Y. Wang, G.Q. Xie, Z.Y. Pu, P. Fang, Y.L. Xie, Preparation and characterization of nanostructured $Ce_{0.9}Cu_{0.1}O_{2-d}$ solid solution with high surface area and its application for low temperature CO oxidation, Catal. Commun. 8 (2007) 834–838.
[17] X. Tang, B. Zhang, Y. Li, Y. Xu, Q. Xin, W. Shen, CuO/CeO_2 catalysts: redox features and catalytic behaviors, Appl. Catal. A 288 (2005) 116–125.
[18] T. Tabakova, V. Idakiev, J. Papavasiliou, G. Avgouropoulos, T. Ioannides, Effect of additives on the WGS activity of combustion synthesized CuO/CeO_2 catalysts, Catal. Commun. 8 (2007) 101–106.
[19] T. Caputo, L. Lisi, R. Pirone, G. Russo, On the role of redox properties of CuO/CeO_2 catalysts in the preferential oxidation of CO in H_2-rich gases, Appl. Catal. A 348 (2008) 42–53.
[20] H.C. Lee, D.H. Kim, Kinetics of CO and H_2 oxidation over CuO–CeO_2 catalyst in H_2 mixtures with CO_2 and H_2O, Catal. Today 132 (2008) 109–116.
[21] J.W. Park, J.H. Jeong, W.L. Yoon, C.S. Kim, D.K. Lee, Y.-K. Park, Y.W. Rhee, Selective oxidation of CO in hydrogen-rich stream over Cu–Ce catalyst promoted with transition metals, Int. J. Hydrogen Energy 30 (2005) 209–220.
[22] F. Marino, C. Descorme, D. Duprez, Supported base metal catalysts for the preferential oxidation of carbon monoxide in the presence of excess hydrogen (PROX), Appl. Catal. B 58 (2005) 175–183.
[23] G. Avgouropoulos, T. Ioannides, H. Matralis, Influence of the preparation method on the performance of CuO–CeO_2 catalysts for the selective oxidation of CO, Appl. Catal. B 56 (2005) 87–93.
[24] I. Rosso, C. Galletti, G. Saracco, E. Garrone, V. Specchia, Development of A zeolites-supported noble-metal catalysts for CO preferential oxidation: H_2 gas purification for fuel cell, Appl. Catal. B 48 (2004) 195–203.
[25] P. Zimmer, A. Tschope, R. Birringer, Temperature-programmed reaction spectroscopy of ceria- and Cu/ceria-supported oxide catalyst, J. Catal. 205 (2002) 339–345.
[26] J.Y. Kim, J.A. Rodriguez, J.C. Hanson, A.I. Frenkel, P.L. Lee, Reduction of CuO and Cu_2O with H_2: H embedding and kinetic effects in the formation of suboxides, J. Am. Chem. Soc. 125 (2003) 10684–10692.
[27] A. Martinez-Arias, M. Fernandez-Garcia, G.J. Soria, J.C. Conesa, Spectroscopic study of a Cu/CeO_2 catalyst subjected to redox treatments in carbon monoxide and oxygen, J. Catal. 182 (1999) 367–377.
[28] M. Fernandez-Garcia, A. Martinez-Arias, A. Iglesias-Juez, C. Belver, A.B. Hungria, J.C. Conesa, J. Soria, Structural characteristics and redox behavior of CeO_2–ZrO_2/Al_2O_3 supports, J. Catal. 194 (2000) 385–392.
[29] A. Martinez-Arias, M. Fernandez-Garcia, O. Galvez, J.M. Coronado, J.A. Anderson, J.C. Conesa, J. Soria, G. Munuera, Comparative study on redox properties and catalytic behavior for CO oxidation of CuO/CeO_2 and CuO/$ZrCeO_4$ catalysts, J. Catal. 195 (2000) 207–216.
[30] A. Martinez-Arias, M. Fernandez-Garcia, A.B. Hungria, A. Iglesias-Juez, O. Galvez, J.A. Anderson, J.C. Conesa, J. Soria, G. Munuera, Redox interplay at copper oxide–(Ce,Zr)O_x interfaces: influence of the presence of NO on the catalytic activity for CO oxidation over CuO/$CeZrO_4$, J. Catal. 214 (2003) 261–272.
[31] A. Martinez-Arias, A.B. Hungria, M. Fernandez-Garcia, J.C. Conesa, G. Munuera, Interfacial redox processes under CO/O_2 in a nanoceria-supported copper oxide catalyst, J. Phys. Chem. B 108 (2004) 17983–17991.
[32] G. Sedmak, S. Hocevar, J. Levec, Transient kinetic model of CO oxidation over a nanostructured $Cu_{0.1}Ce_{0.9}O_{2-y}$ catalyst, J. Catal. 222 (2004) 87–99.
[33] A. Dandekar, M.A. Vannice, Determination of the dispersion and surface oxidation states of supported Cu catalysts, J. Catal. 178 (1998) 621–639.
[34] M.H. Kim, J.R. Ebner, R.M. Friedman, M.A. Vannice, Determination of metal dispersion and surface composition in supported Cu–Pt catalysts, J. Catal. 208 (2002) 381–392.
[35] W. Liu, M. Flytzany-Stephanopoulos, Total oxidation of carbon-monoxide and methane over transition metal fluorite oxide composite catalysts. II. Catalyst characterization and reaction-kinetics, J. Catal. 153 (1995) 317–322.